Journal of Hazardous Materials 171 (2009) 459–464

Contents lists available at ScienceDirect

Journal of Hazardous Materials

journal homepage: www.elsevier.com/locate/jhazmat

Using shell-tunable mesoporous Fe_3O_4@HMS and magnetic separation to remove DDT from aqueous media

Hua Tian [a], Jinjun Li [a], Qun Shen [a], Hailin Wang [a], Zhengping Hao [a,*], Linda Zou [b], Qin Hu [a]

[a] Department of Environmental Nano-materials, Research Center for Eco-Environmental Sciences, Chinese Academy of Sciences, Beijing 100085, China
[b] Center for Water Management and Reuse, University of South Australia, South Australia 50951, Australia

ARTICLE INFO

Article history:
Received 1 November 2008
Received in revised form 20 May 2009
Accepted 6 June 2009
Available online 16 June 2009

Keywords:
DDT
Magnetic separation
HMS
Magnetic mesoporous silica

ABSTRACT

1,1-bis(4-chlorophenyl)-2,2,2-trichloroethane (DDT) is of concern in water treatment because of its persistence and health effects. A new concept is proposed to synthesize hexagonal mesoporous silica (HMS) with magnetic functionalization for DDT removal from aqueous media. Fe_3O_4 nanocrystals were synthesized by a low-temperature solvothermal process, and then encapsulated in mesoporous silica through a packing approach, forming core–shell structured Fe_3O_4@HMS microspheres. The synthesized materials were characterized by X-ray diffraction (XRD), transmission electron microscopy (TEM) and nitrogen adsorption–desorption techniques. The results indicate that the silica shell conserves mesoporous structure after the removal of surfactant templates. Different from previous studies, the thickness, pore volume and surface area of silica shell can be controlled by adjusting the reaction condition. These Fe_3O_4@HMS materials show high adsorption capacity and fast adsorption rate for DDT. Because of the useful magnetic property and unique mesoporous structure, the synthesized materials provide a fast, convenient and highly efficient means to remove DDT from aqueous media.

Crown Copyright © 2009 Published by Elsevier B.V. All rights reserved.

1. Introduction

DDT has been used extensively as a broad-spectrum pesticide for agricultural and residential purpose and in public health programs. Because of concerns about its toxicity and persistence, many countries banned or restricted the use of DDT in the 1970s. However, chemical stability and associated lipophilicity result in high DDT accumulation in environment media [1–3] and in human tissues [4]. DDT residues affect the central neural systems, produce microscopic changes in the liver and kidneys, and cause reproductive disorders [5].

Many methods for removing DDT from water have been studied, including biological treatments [6], photochemical reactions [7] and reductive dechlorination [8]. However, many limitations such as lower efficiency, long reaction time and rigorous reaction condition, even toxic byproducts produced, exist. These limitations have inhibited their applications in the actual environment. Compared with these methods mentioned above, adsorption has been found to be an effective, simple and environmental friendly method. Various adsorbents, such as activated carbon, polymeric resins and organoclays, have been explored for the removal of DDT and other pesticides from water [9–11]. These materials, however, generally display poor adsorption efficiency or low uptake affinity toward organic molecules.

Due to their large surface area, tunable porosity, uniform pore size distribution, controlled morphology and high thermal stability, mesoporous silicas have been demonstrated to be good effective adsorbents of volatile organic compounds (VOCs), biomolecules and pesticides [12–15]. For many applications, small particle sizes are advantageous, but are not convenient to be separated from the liquid phase after use. In addition, compared with microporous zeolites, the hydrothermal stability of these mesoporous silicas is relatively low [16], which severely hinders their practical applications in aqueous environment, especially for some applications with long reaction time.

Recently, magnetic mesoporous silicas attracted considerable attention for the combined functionalities of mesoporous structure and sufficient magnetization [17,18]. These composites possess a network of channels and voids of well-defined size in nanoscale range, which makes them suitable candidates for hosting a variety of molecules. The magnetic characteristics make the separation treatment convenient in liquid-phase processes by applying an external magnetic field. So far, magnetic mesoporous silica materials have shown great potential in various fields [19–21], being considered as ideal hosts for protein and microcystins in aqueous solution. However, there are few reports on the potential for the removal of organic pollutions. Meanwhile, previous studies are mainly focused on increasing the magnetization value of the samples or controlling the distribution of magnetic particles in

* Corresponding author. Tel.: +86 10 62923564; fax: +86 10 62923564.
E-mail address: zpinghao@rcees.ac.cn (Z. Hao).

0304-3894/$ – see front matter. Crown Copyright © 2009 Published by Elsevier B.V. All rights reserved.
doi:10.1016/j.jhazmat.2009.06.029

the composites. It is desirable and significant to prepare magnetic mesoporous silica materials with controllable surface area, tunable shell thickness for adsorption and separation applications.

Researches for preparation of magnetic mesoporous materials were centered on three approaches: (i) dispersing magnetic nanoparticles in the pores of mesoporous silicas [22]; (ii) grafting magnetic nanoparticles on the outer surface of mesoporous silicas [17]; (iii) coating mesoporous silicas onto the monodisperse magnetic nanoparticles to compose core–shell structured microspheres [23]. Compared with the synthesis methods of (i) and (ii), coating mesoporous silicas onto the monodisperse magnetic nanoparticles can provide uniform shape and size that are favorable for them to respond to magnetic field well, and produce the materials with higher surface area and pore volume, which are beneficial to the adsorption process [24,25]. Therefore, the coating method was chosen in this work to synthesize a novel magnetic mesoporous silica material consisting of Fe_3O_4 core and hexagonal mesoporous silica (HMS) shell. The properties of the obtained materials were characterized by XRD, TEM, FT-IR and nitrogen adsorption–desorption. By studying the DDT adsorption in aqueous media, we investigated the adsorption kinetics and capacity of these materials to clarify their potential applications as organic molecule carriers. The affinity of the synthesized materials toward DDT was also evaluated.

2. Experimental

2.1. Chemicals

The following chemicals were used without further purification: DDT (Aldrich); *n*-hexane (HPLC, Tedia Company, USA); dodecylamine (Sinopharm Chemical Reagent Co., Ltd., China). All other chemicals were purchased from Beijing Chemical Reagent Factory. Sodium sulphate (Na_2SO_4) was oven-dried at 150 °C for 2 h to act as a desiccant.

2.2. Synthesis of magnetic Fe_3O_4 nanoparticles

Fe_3O_4 particles were synthesized by a solvothermal reaction. In a typical synthesis, 2.70 g of $FeCl_3{\cdot}6H_2O$ and 6.76 g of CH_3COONH_4 were mixed in 100 mL of ethylene glycol. After stirring for 1.0 h by a magnetic stirrer (HJ-2, Guohua Electric Appliance Co., Ltd.), the solution was poured into a Teflon-lined stainless autoclave (200 mL). The autoclave was sealed and heated at 200 °C for 12 h. The resulting product was cooled down to room temperature, and washed with ethanol for five times, and finally dried in vacuum at 70 °C for 3 h.

2.3. Synthesis of magnetic mesoporous Fe_3O_4@HMS

Briefly, 0.50 g of Fe_3O_4 particles were dispersed in 250 mL of 0.1 M HCl aqueous solution by ultrasonication for 10 min, and then separated and washed with deionized water. 0.35 g of dodecylamine was dissolved into a mixture of 3.94 g of ethanol and 27.36 g of H_2O. Then the as-treated Fe_3O_4 particles were added into the system. After vigorous stirring for 0.5 h, 2.0 g of tetraethylorthosilicate (TEOS) was added dropwise to the mixed solution. The reaction mixture was then stirred at ambient temperature for 24 h, collected with a magnet and washed with deionized water and ethanol to remove nonmagnetic by-products. Finally, the resulting powders were extracted by refluxing with 200 mL ethanol at 80 °C for 24 h. The extraction was repeated for twice to remove the surfactant templates completely. Finally, the product was washed with deionized water, and denoted as Fe_3O_4@HMS-1.

For increasing the thickness of silica shell, the extraction processes mentioned above were varied while keeping other reaction conditions constant. The resulting powders before refluxing extraction were redispersed in a mixed solution containing of dodecylamine (0.35 g), ethanol (3.94 g) and H_2O (27.36 g). After 0.5 h stirring, 2 g of TEOS was introduced. The mixture was stirred for 24 h, collected with a magnet and washed repeated by deionized water and ethanol. Finally, the product was extracted with ethanol as above mentioned, then washed with deionized water and named as Fe_3O_4@HMS-2.

For comparison, some HMS samples were synthesized by employing slightly modified the above procedures. 4 g of TEOS was dissolved into a mixture of water 54.72 g, dodecylamine 0.70 g and ethanol 7.88 g under vigorous stirring. The mixture was stirred for 24 h, and then filtered, washed with distilled water and ethanol. The product was extracted with ethanol as above mentioned, and then washed with deionized water.

2.4. Characterization

XRD measurement was performed on a Siemens D5005 X-ray diffractometer using Cu Kα radiation (40 mA, 40 kV). TEM images were obtained using a Hitachi H-7500 microscope. A typical TEM sample was prepared by depositing several droplets of the nanoparticles/ethanol mixture onto a carbon-coated Cu-grid. Fourier-transform infrared (FT-IR) spectra were recorded on a Bruker Tensor 27 spectrometer in the range of 600–4000 cm^{-1} at a resolution of 4 cm^{-1}. The textural properties of materials were measured by nitrogen adsorption–desorption at liquid nitrogen temperature, using a gas sorption analyzer NOVA 1200. Magnetization measurements were performed on a Lake Shore 7307 Vibrating sample magnetometer.

2.5. DDT adsorption

DDT adsorptions were conducted in water–acetone (9:1, v/v) phase. Acetone is known as a solubilizing agent [26]. 10 mg of samples of Fe_3O_4@HMS-2 were placed into 40 mL glass vials and 35 mL of the DDT aqueous solution with desired concentration (diluted from 100 μg mL^{-1}) was added in each vial. Reaction vials were tightly sealed with Teflon-lined screw caps to prevent any loss of solution. To minimize the aggregation of adsorbent and decrease the influence of diffusion on the DDT adsorption rate, vials were shaken continuously at room temperature. At predetermined time intervals, vials were removed from the shaker and separated with the help of a magnet. 20 mL of supernatant solution was removed and extracted with *n*-hexane to recover DDT. 1 mL aliquots of the hexane extracts were removed in 2 mL glass vials for GC–MS analysis to confirm the residual DDT concentration.

2.6. GC–MS analysis

GC–MS analysis was conducted on an Agilent 6890 gas chromatograph equipped with an Agilent 5973 mass selective detector. HP-5 capillary column (0.25 μm, 0.25 mm × 30 m) was used with ultra high purity helium as the carrier gas. The initial temperature of run was maintained at 70 °C for 2 min, increased at 20 °C/min to 200 °C and at 10 °C/min to 280 °C, and maintained at the final temperature for 1.5 min. The net run time for the analysis was 18 min.

3. Results and discussion

3.1. Features of materials

Fig. 1 provides the low-angle XRD patterns of as-synthesized Fe_3O_4, Fe_3O_4@HMS-1 and Fe_3O_4@HMS-2, respectively. After coating SiO_2, the samples exhibit single d_{100} reflections, confirming

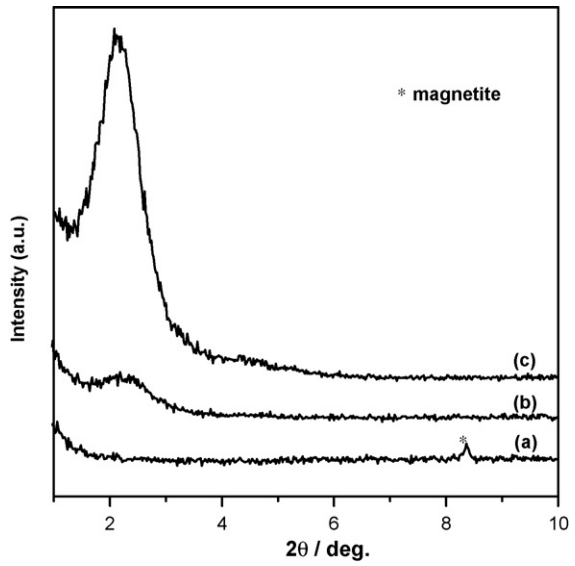

Fig. 1. Low-angle XRD patterns of Fe_3O_4 (a), Fe_3O_4@HMS-1 (b) and Fe_3O_4@HMS-2 (c).

short-range hexagonal symmetry of the materials, and an ordered mesoporous HMS formed [27]. The intensity of this peak becomes stronger, and it is shifted to lower angles with increasing amount of HMS coated (sample Fe_3O_4@HMS-2), indicating that a lattice expansion occurred and the mesoporous structure is affected by the amount of HMS coated. Wide-angle XRD patterns (Fig. 2) show that the materials have diffraction peaks similar to that of the parent Fe_3O_4 particles, suggesting that the Fe_3O_4 particles were well retained in the silica matrix. The broad band centered at $2\theta = 22^\circ$ can be assigned to the characteristic reflection from amorphous SiO_2 (JCPDS 29-0085). With increasing the coated HMS amount, the intensities of all Fe_3O_4 diffraction peaks decrease apparently, while the diffraction peak of SiO_2 increases, demonstrating that more amount of HMS is undoubtedly coated on the surface of Fe_3O_4, which can be further confirmed by their TEM images.

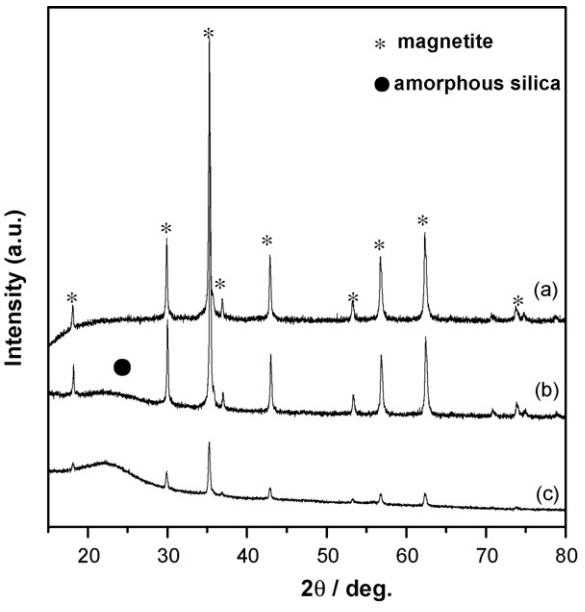

Fig. 2. Wide-angle XRD patterns of Fe_3O_4 (a), Fe_3O_4@HMS-1 (b) and Fe_3O_4@HMS-2 (c).

Fig. 3 shows the TEM images of samples. The initial Fe_3O_4 particles are uniform with a mean diameter of about 350 nm. These uniform cores can produce a narrow distribution of the final particle sizes. The TEM image of Fe_3O_4@HMS-1 shows a core–shell structure with a thin HMS layer (ca. 15 nm in thickness) is clearly obtained. The shell thickness is easily tuned up to ca. 40 nm (Fig. 3c) by varying the amount of TEOS/dodecylamine mixture. The higher magnification TEM images (Fig. 3b and c) represent that all Fe_3O_4@HMS composites have disordered wormhole-like frameworks, which are typical of HMS wormhole structures assembled from long alkyl chain neutral amines as surfactants [28].

The physical adsorption–desorption of nitrogen is an effective technique for determining the textural properties of mesoporous materials. The nitrogen adsorption–desorption isotherms and pore size distribution profiles of the Fe_3O_4@HMS samples with various shell thickness are shown in Fig. 4. These Fe_3O_4@HMS samples show type IV isotherm and a narrow pore size distribution, similar to those of HMS materials reported by other authors [28,29]. Two capillary condensation steps are observed on the adsorption–desorption isotherms of these materials. The first hysteresis loop at lower relative pressure (near $P/P_0 = 0.15$) indicates the presence of framework mesoporosity, and the second hysteresis loop at higher relative pressure (near $P/P_0 = 0.90$) is due to textural interparticle mesoporosity or macroporosity [28]. This clearly indicates that the Fe_3O_4@HMS composites exhibit, in addition to the framework-confined porosity (structural porosity), a textural porosity. In addition, the hysteresis loop becomes broader and shifts to higher pressure with increasing the coated HMS amount, which shows the changes of the pore volume and pore diameter. After increasing the coated HMS amount, the BET surface area ($283.3\ m^2\ g^{-1}$) and pore volume ($0.221\ cm^3\ g^{-1}$) increased to $769.9\ m^2\ g^{-1}$ and $0.666\ cm^3\ g^{-1}$, respectively. The pore diameter also slightly increased from 3.1 to 3.5 nm. It can be expected that Fe_3O_4@HMS-2 possesses high adsorption capability as an organic molecule carrier for the organic pollutant targeting system.

Fig. 5 shows IR spectra of HMS and Fe_3O_4@HMS. For the HMS sample, the absorption peak at $1050\ cm^{-1}$ is corresponded to the Si–O asymmetrical stretching of siloxane [19], becoming stronger after loading Fe_3O_4. This can be ascribed to the interaction between the Fe_3O_4 and Si–O, which may form the Fe–O–Si bond. A new peak at $1298\ cm^{-1}$ assigned to the Fe–O vibration is observed in the spectrum of Fe_3O_4@HMS-2. The sharp peak at $964\ cm^{-1}$ present in pristine HMS silica increases upon loading with Fe_3O_4. More evidence, in that a very similar band is observed in mixed oxides [30] or in mixed oxides grafted on silica [31], supports that the characteristic band is due to a modification of SiO_4 units indirectly related to the presence of heterometals. Therefore, the adsorption peak at $964\ cm^{-1}$ is rather a fingerprint of the heteroatom Fe on the matrix of [SiO_4] units. Thus, we can conclude that Fe_3O_4 has been incorporated into the Fe_3O_4@HMS mainly by the Fe–O–Si bond formed between the Fe_3O_4 and Si–O of siloxane or SiO_4 units.

The hysteresis loops of the prepared samples were registered at 300 K. The field-dependent magnetization plots illustrate these samples are magnetic at room temperature (Fig. 6). The saturation magnetization value of Fe_3O_4 is $81.2\ emu\ g^{-1}$, but it dramatically decreases to $49.7\ emu\ g^{-1}$ for Fe_3O_4@HMS-1, and $8.0\ emu\ g^{-1}$ for Fe_3O_4@HMS-2, which confirms that the magnetization values of Fe_3O_4@HMS can be tunable by controlling the silica content of magnetic mesoporous spheres. Although the magnetization curves show hysteresis, the remanent magnetization values are very small, $0.2\ emu\ g^{-1}$ for Fe_3O_4@HMS-2. The Fe_3O_4@HMS with magnetic characteristics and high magnetization values can quickly respond to the external magnetic field and re-disperse once the external magnetic field is removed. This is advantageous for the separation and purification applications.

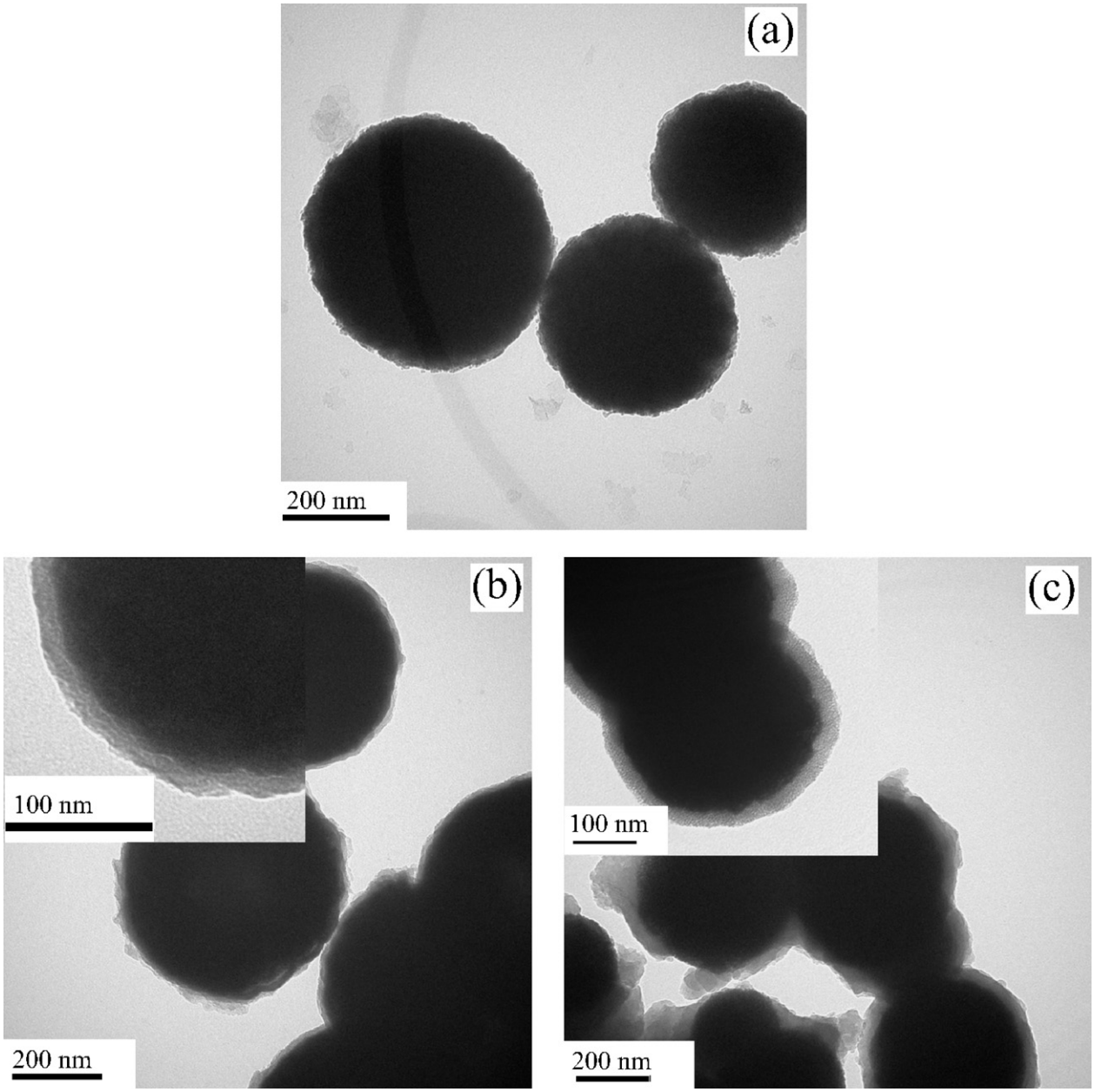

Fig. 3. TEM images of Fe_3O_4 (a), Fe_3O_4@HMS-1 (b) and Fe_3O_4@HMS-2 (c).

3.2. DDT adsorption

To explore the adsorption and separation abilities of Fe_3O_4@HMS, we investigated the applicability for the DDT removal by these magnetic mesoporous silica spheres. Fig. 7 shows the time profile of DDT removal with these magnetic mesoporous silica spheres. The first point versus time 0 h represents the blank sample, determined before the addition of Fe_3O_4@HMS-2. It is noteworthy that the DDT adsorption is a rapid process with almost 90% DDT being removed within approximately 0.25 h, indicating a high affinity between the DDT molecules and the mesoporous silica of microspheres. Afterwards, the adsorption rate slows and then reaches the equilibrium after approximately 1.0 h. To evaluate the adsorption capability of Fe_3O_4@HMS, several experiments with different initial DDT concentrations were conducted for the comparisons of adsorption amount and efficiency. Fig. 8 shows that with increasing the initial DDT concentration, the removal efficiency initially rises, then decreases slightly, and finally reaches a plateau. However, the adsorption amount shows continuous increase in our tested concentration range of DDT, suggesting high adsorption capability of these magnetic mesoporous silica materials. Mesoporous HMS without the incorporation of Fe_3O_4 was employed for comparison at the same experimental conditions. It was found that the adsorption amount of DDT on HMS materials was only 2.77 $\mu g\,mg^{-1}$ with the initial DDT concentration 2.2 $\mu g\,mL^{-1}$, much lower than that of Fe_3O_4@HMS-2 (ca. 7.5 $\mu g\,mg^{-1}$).

It is reported that the effectiveness of an adsorbent to remove a given ion or molecule can be expressed in terms of a distribution coefficient, K_d [15,32],

$$K_d = \frac{(C_0 - C)V}{Cm} \quad (1)$$

where C_0 and C are the initial and final DDT concentrations, V is the solution volume (mL) and m is the adsorbent amount (g). The K_d values of Fe_3O_4@HMS-2 and HMS toward DDT were measured using

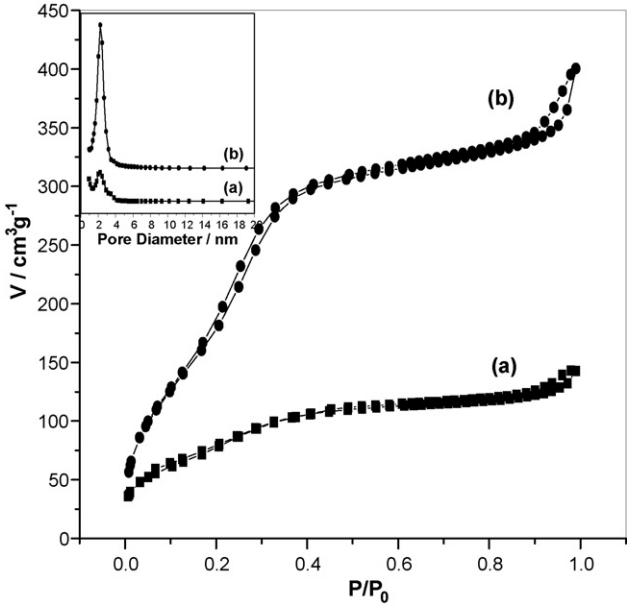

Fig. 4. N_2 adsorption–desorption isotherms and pore size distribution (inset) of Fe_3O_4@HMS samples: (a) Fe_3O_4@HMS-1 and (b) Fe_3O_4@HMS-2.

their respective adsorption data with the same experiment condition. The results indicate that the K_d value of Fe_3O_4@HMS-2 is about 130×10^3 mL g^{-1}, much higher than that of HMS (10×10^3 mL g^{-1}). This corroborates the especially high affinity of Fe_3O_4@HMS toward DDT.

Compared with HMS, higher adsorption capability and stronger uptake affinity of Fe_3O_4@HMS-2 toward DDT can be attributed to its numerous accessible pores and the slight surfactant templates retained in its pore channels, which enhance the uptake affinity toward organic molecules [14].

Fig. 9 displays a representative separation process of Fe_3O_4@HMS-2 from DDT aqueous solution. A low dose of these microspheres was used. It indicated that the microspheres in their homogeneous dispersion show fast movement to the applied magnetic field, suggesting the Fe_3O_4@HMS-2 microspheres possess

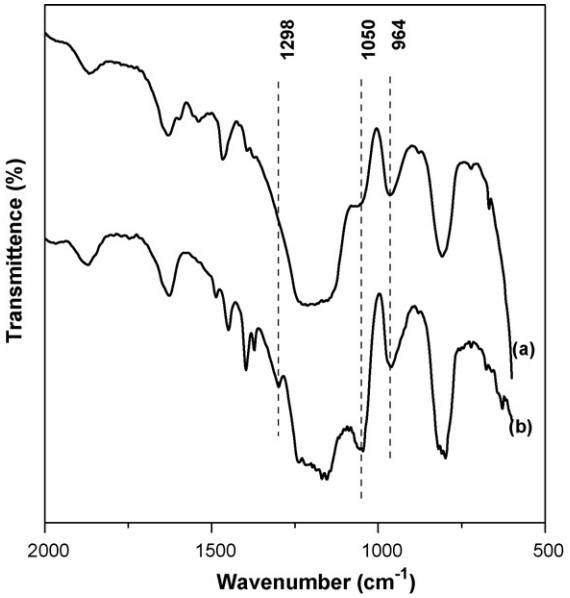

Fig. 5. The FT-IR spectra of HMS (a) synthesized by the ethanol extraction and Fe_3O_4@HMS-2 (b).

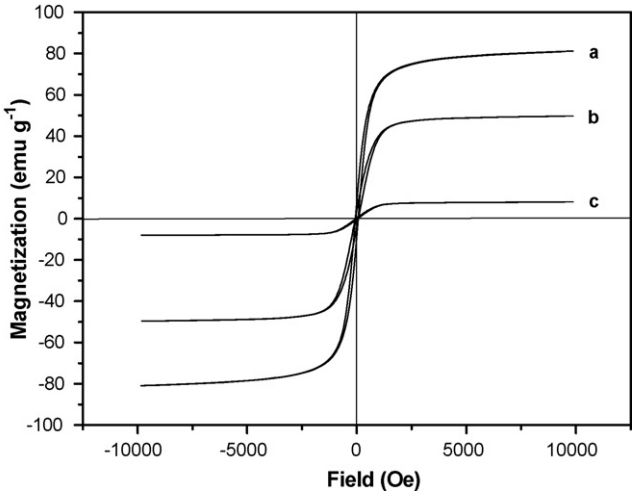

Fig. 6. The magnified hysteresis loops as a function of applied magnetic field measured at 300 K: (a) Fe_3O_4, (b) Fe_3O_4@HMS-1 and (c) Fe_3O_4@HMS-2.

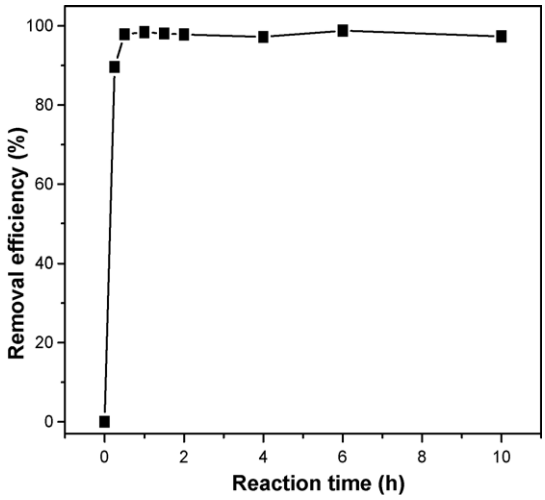

Fig. 7. Removal efficiency of DDT on Fe_3O_4@HMS-2. Experimental conditions: initial DDT 2.88 μg mL^{-1}, Fe_3O_4@HMS-2 0.28 mg mL^{-1}.

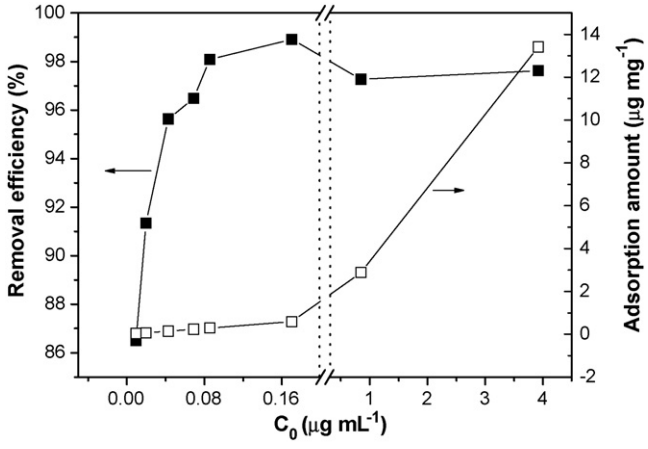

Fig. 8. Impact of initial concentration on DDT adsorption amount and efficiency on Fe_3O_4@HMS-2.

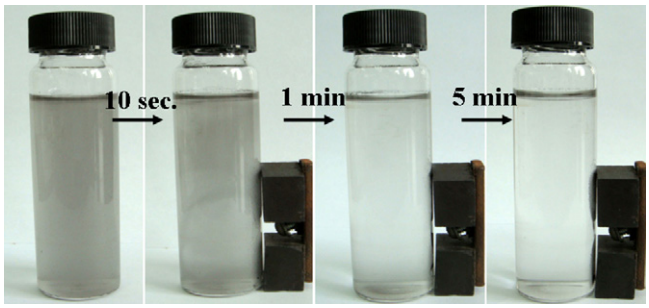

Fig. 9. The magnetic separation process of Fe_3O_4@HMS-2 after DDT adsorption.

excellent magnetic responsivity, which is an advantage to their practical applications.

4. Conclusions

A novel kind of magnetic materials with a Fe_3O_4 core and mesoporous HMS shell has been successfully fabricated. The Fe_3O_4 nanocrystals were loaded in the mesoporous silica matrix of HMS by Fe–O–Si band. The shell thickness, pore volume and surface area of silica shell can be tuned by adjusting the amount of silica source and reaction process. Through the investigation of DDT adsorption on magnetic mesoporous silica spheres, it was found that these materials could be an excellent adsorbent for fast and highly efficient removal of DDT from aqueous media. Because of the unique mesoporous structure and magnetic properties, these magnetic silica materials can offer a very convenient and useful means for the removal of organic pollutants.

Acknowledgements

This work was financially supported by the National Science Fund of China (20725723, 20807050) and National High Technology Research & Development Program of China (2006AA06A310) is gratefully acknowledged.

References

[1] X.L. Yang, S.S. Wang, Y.R. Bian, F. Chen, G.F. Yu, C.G. Gu, X. Jiang, Dicofol application resulted in high DDTs residue in cotton fields from northern Jiangsu province, China, J. Hazard. Mater. 150 (2008) 92–98.
[2] T. Poolpak, P. Pokethitiyook, M. Kruatrachue, U. Arjarasirikoon, N. Thanwaniwat, Residue analysis of organochlorine pesticides in the Mae Klong river of Central Thailand, J. Hazard. Mater. 156 (2008) 230–239.
[3] R.O. Yang, T.D. Yao, B.Q. Xu, G.B. Jiang, X.D. Xin, Accumulation features of organochlorine pesticides and heavy metals in fish from high mountain lakes and Lhasa River in the Tibetan Plateau, Environ. Int. 33 (2007) 151–156.
[4] D. Carrizo, J.O. Grimalt, N. Ribas-Fito, J. Sunyer, M. Torrent, Physical–chemical and maternal determinants of the accumulation of organochlorine compounds in four-year-old children, Environ. Sci. Technol. 40 (2006) 1420–1426.
[5] US Department of Health and Services, Toxicological profile for DDT, DDE and DDD, Agency for Toxic Substances and Disease Registry, Atlanta, GA, September 2002.
[6] M. Douglase, R. Boakaik, A. Martin, Bioavailability to earthworms of aged DDT, DDE, DDD, and deldrin in soil, Environ. Sci. Technol. 34 (2000) 709–713.
[7] W. Chu, Photodechlorination mechanism of DDT in a UV/surfactant system, Environ. Sci. Technol. 33 (1999) 421–425.
[8] G.D. Sayles, G. You, M. Wang, M.J. Kuperferle, DDT, DDD, and DDE dechlorination by zero-valent iron, Environ. Sci. Technol. 31 (1997) 3448–3454.
[9] J.M. Stuart, R.F. Neil, Supercritical adsorption and desorption behavior of DDT on activated carbon using carbon dioxide, Ind. Eng. Chem. Res. 34 (1995) 275–282.
[10] N. Masque, M. Galia, R.M. Marce, F. Borrull, New chemically modified polymeric resin for solid-phase extraction of pesticides and phenolic compounds from water, J. Chromatogr. A 803 (1998) 147–155.
[11] J. Lemic, D. Kovacevic, M. Tomasevic-Canovic, D. Kovacevic, T. Stanic, R. Pfend, Removal of atrazine, lindane and diazinone from water by organo-zeolites, Water Res. 40 (2006) 1079–1085.
[12] J.W. Lee, J.W. Lee, W.G. Shim, S.H. Suh, H. Moon, Adsorption of chlorinated volatile organic compounds on MCM-48, J. Chem. Eng. Data 48 (2003) 381–387.
[13] A. Katiyar, S. Yadav, P.G. Smirniotis, N.G. Pinto, Synthesis of ordered large pore SBA-15 spherical particles for adsorption of biomolecules, J. Chromatogr. A 1122 (2006) 13–20.
[14] P.A. Mangrulkar, S.P. Kamble, J. Meshram, S.S. Rayalu, Adsorption of phenol and *o*-chlorophenol by mesoporous MCM-41, J. Hazard. Mater. 160 (2008) 414–421.
[15] R. Sawicki, L. Mercier, Evaluation of mesoporous cyclodextrin-silica nanocomposites for the removal of pesticides from aqueous media, Environ. Sci. Technol. 40 (2006) 1978–1983.
[16] F.S. Xiao, Ordered mesoporous materials with improved stability and catalytic activity, Top. Catal. 35 (2005) 9–24.
[17] A.H. Lu, W.C. Li, A. Kiefer, W. Schmidt, E. Bill, G. Fink, F. Schuth, Fabrication of magnetically separable mesostructured silica with an open pore system, J. Am. Chem. Soc. 126 (2004) 8616–8617.
[18] P. Wu, J. Zhu, Z. Xu, Template-assisted synthesis of mesoporous magnetic nanocomposite particles, Adv. Funct. Mater. 14 (2004) 345–351.
[19] S. Huang, P. Yang, Z. Cheng, C. Li, Y. Fan, D. Kong, J. Lin, Synthesis and characterization of magnetic Fe_xO_y@SBA-15 composites with different morphologies for controlled drug release and targeting, J. Phys. Chem. C 112 (2008) 7130–7137.
[20] S. Giri, B.G. Trewyn, M.P. Stellmaker, V.S.Y. Lin, Stimuli-responsive controlled-release delivery system based on mesoporous silica nanorods capped with magnetic nanoparticles, Angew. Chem. Int. Ed. 44 (2005) 5038–5044.
[21] Y. Deng, D. Qi, C. Deng, X. Zhang, D. Zhao, Superparamagnetic high-magnetization microspheres with an Fe_3O_4@SiO_2 core and perpendicularly aligned mesoporous SiO_2 shell for removal of microcystins, J. Am. Chem. Soc. 130 (2008) 28–29.
[22] A.F. Gross, M.R. Diehl, K.C. Beverly, E.K. Richman, S.H. Tolbert, Controlling magnetic coupling between cobalt nanoparticles through nanoscale confinement in hexagonal mesoporous silica, J. Phys. Chem. B 107 (2003) 5475–5482.
[23] W. Zhao, J. Gu, L. Zhang, H. Chen, J. Shi, Fabrication of uniform magnetic nanocomposite spheres with a magnetic core/mesoporous silica shell structure, J. Am. Chem. Soc. 127 (2005) 8916–8917.
[24] S.C. Tsang, C.H. Yu, H. i Tang, H. He, V. Castelletto, I.W. Hamley, T. Narayanan, C.C.H. Lo, K. Tam, Assembly of centimeter long silica coated FePt colloid crystals with tailored interstices by magnetic crystallization, Chem. Mater. 20 (2008) 4554–4556.
[25] J. Kim, J.E. Lee, J. Lee, J.H. Yu, B.C. Kim, K. An, Y. Hwang, C.H. Shin, J.G. Park, J. Kim, T. Hyeon, Magnetic fluorescent delivery vehicle using uniform mesoporous silica spheres embedded with monodisperse magnetic and semiconductor nanocrystals, J. Am. Chem. Soc. 128 (2006) 688–689.
[26] S.K. Gautam, S. Suresh, Studies on dechlorination of DDT (1,1,1-trichloro-2,2-bis(4-chlorophenyl)ethane) using magnesium/palladium bimetallic system, J. Hazard. Mater. 139 (2007) 146–153.
[27] T.A. Zepeda, J.L.G. Fierro, B. Pawelec, R. Nava, T. Klimova, G.A. Fuentes, T. Halachev, Synthesis and characterization of Ti-HMS and CoMo/Ti-HMS oxide materials with varying Ti content, Chem. Mater. 17 (2005) 4062–4073.
[28] T.R. Pauly, Y. Liu, T.J. Pinnavaia, S.J.L. Billinge, T.P. Rieker, Textural mesoporosity and the catalytic activity of mesoporous molecular sieves with wormhole framework structures, J. Am. Chem. Soc. 121 (1999) 8835–8842.
[29] P.T. Tanev, T.J. Pinnavaia, Mesoporous silica molecular sieves prepared by ionic and neutral surfactant templating: a comparison of physical properties, Chem. Mater. 8 (1996) 2068–2079.
[30] Z. Liu, R.J. Davis, Investigation of the structure of microporous Ti–Si mixed oxides by X-ray, UV reflectance, FT-Raman, and FT-IR spectroscopies, J. Phys. Chem. 98 (1994) 1253–1261.
[31] S. Srinivasan, A.K. Datye, M. Hampden Smith, I.E. Wachs, G. Deo, J.M. Jehng, A.M. Turek, C.H.F. Peden, The formation of titanium oxide monolayer coatings on silica surfaces, J. Catal. 131 (1991) 260–275.
[32] M.C. Burleigh, S. Dai, E.W. Hagaman, J.S. Lin, Imprinted polysilsesquioxanes for the enhanced recognition of metal ions, Chem. Mater. 13 (2001) 2537–2546.